Experimental testing of a dew point evaporative cooler: Test bench architecture and commissioning

Alanis Zeoli [a], Bernard Loly [a], Anna Pacak [b], Vincent Lemort [a], Samuel Gendebien [a]*

[a] *Laboratory of Applied Thermodynamics, Department of Aerospace and Mechanical Engineering, University of Liège, Belgium*
[*] *Corresponding author: alanis.zeoli@uliege.be*

Abstract:
Evaporative cooling technologies rely on the cooling effect occurring during water evaporation. They are a promising solution to address the drawbacks of vapour-compression systems, including their harmful environmental impact, and to reduce the energy demand for air conditioning in buildings. In this work, a test-bench architecture and its commissioning steps have been presented to enable testing of a dew-point indirect evaporative cooling device. It is equipped with a thermocouple grid that monitors the evaporative cooler's performance homogeneity. It was found that applying a trade-off in water management may enhance the energy performance of evaporative coolers, as a low water supply might cause the wet channel to dry out and decrease heat transfer between the primary and secondary sides, while a high water supply can result in channel flooding. The test bench enables simulation of inlet conditions across different climatic zones and monitoring of air conditions at the device's inlet and outlet, both of which are valuable for validating mathematical models.

Keywords:
Evaporative cooling; Alternative cooling, Passive cooling, Sustainable cooling; Experimental data

1. Introduction

1.1. Context

Over the past few decades, energy consumption for air conditioning has risen [1], driven by improvements in living standards [2], [3], an ageing population [4], urbanisation [5], and climate change [6]-[9]. The International Energy Agency (IEA) identifies the increasing demand for space cooling as a significant challenge in global energy management [10]. Evaporative cooling technologies (ECTs) are a sustainable alternative to conventional vapour-compression air-conditioning systems. ECTs make use of the latent heat of water vaporisation to lower the air temperature [11], [12] by heat and mass transfer between humid air and a water film. During evaporation, water absorbs heat from the surrounding air, thereby lowering the air temperature. Unlike commonly used vapour-compression systems, ECTs do not require synthetic refrigerants, which contribute notably to global warming through atmospheric leakage [13]. Additionally, because ECTs do not rely on outdoor units that reject heat, they can help reduce the urban heat island effect.

1.2. Principle of indirect evaporative cooling

Dew point indirect evaporative coolers (D-IECs) are a category of evaporative coolers that allow cooling an airstream without humidifying it [14]. D-IECs are composed of alternating dry and wet channels. The primary air flows in the dry channels, where it is cooled only by sensible heat transfer through direct contact with the cold, impermeable wall separating the dry and wet channels. The evaporative cooling process occurs in the wet channels, where secondary air experiences adiabatic cooling due to water evaporation and sensible heating through convective heat transfer between the wall and the airflow.

In the D-IEC, part of the outlet primary air is diverted and redirected to the wet channels to serve as the secondary airflow (Figure 1). The main advantage of this configuration is that it theoretically decreases the minimum achievable temperature to the dew point of the inlet primary air [15]. A higher recirculation rate results in lower outlet temperatures but reduces the airflow of the useful cold air produced. There exists an optimum recirculation rate to maximise the cooling capacity of the D-IEC. It is usually around 30% [16].

In building cooling applications, the primary air is mainly extracted from the indoor environment. To avoid building depressurisation, 70% of the primary air is indoor air (IA), while the remaining 30% is outdoor air (OA). At the D-IEC outlet, 70% of the produced cold air is reinjected into the indoor environment as supply air (SA), while the remaining 30% is redirected to the wet channels as return air (RA). At the D-IEC secondary outlet, warm, humid exhaust air (EA) is discharged to the outdoor environment. The D-IEC performance depends on outdoor air conditions only to a limited extent, as most of the airflow comes from the conditioned indoor environment.

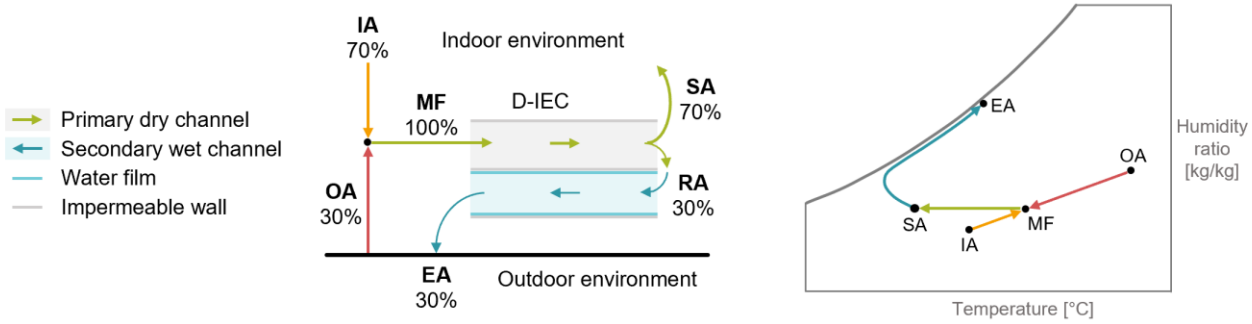

Figure 1. *Integration of a D-IEC in a building and evolution of the air conditions in a psychrometric chart. IA = indoor air, OA = outdoor air, MF = mixed flow, SA = supply air, RA = return air, EA = exhaust air.*

1.3. Goal of the paper

In a previous work [17], the authors identified knowledge gaps in experimental data for validating evaporative cooler models. They established that for the D-IEC configuration, there is currently no dataset that enables model validation on the primary *and* secondary sides. Although most experimental studies measure the temperature and humidity at the primary inlet, primary outlet and secondary outlet to perform energy balance, those measurements are not clearly provided in the papers [18]-[21].

The authors aimed to fill that knowledge gap by experimentally testing a D-IEC under various operating conditions. This paper is intended as a roadmap, detailing the main issues encountered during test-bench design and the first experimental campaign, and could serve as a basis for future experimental research in air-to-air heat exchangers. Section 2 describes the objectives of the test bench and how they translate into constraints for test bench design. The final test bench architecture is shown, and the main components and the monitoring system are described. Section 3 focuses on test bench commissioning, describing the tests performed to ensure proper operation. Finally, Section 4 summarises the first experimental results and raises any encountered problems to identify future research questions.

2. Test bench description

2.1. Objectives of the test bench

The test bench has been designed to obtain a comprehensive dataset for model validation of a dew-point indirect evaporative cooler. The dataset should include experimental measurements of the temperature and humidity at the D-IEC inlet and outlet under various operating conditions, including temperature, humidity and airflow rate. This section describes how this goal translates into constraints for the test bench design.

2.1.1. Description of the tested D-IEC

The internal structure of the D-IEC consists of alternating dry and wet channels, as illustrated in Figure 2. The primary air enters the D-IEC in dedicated dry channels and exits at the back of the D-IEC. There, all the

channels are visible because the primary air outlet corresponds to the secondary air inlet. Part of the primary air is extracted by a fan, but the rest is sucked back into the wet channels by a second fan. The secondary air flows through the D-IEC in the other direction until it reaches the primary inlet. At the entrances of the primary channels, the wet channel walls were sealed to prevent mixing of primary and secondary air. Instead, the outlet opens onto the air collectors, which are perpendicular to the channels and direct the secondary airflow to the top and bottom of the evaporative cooler.

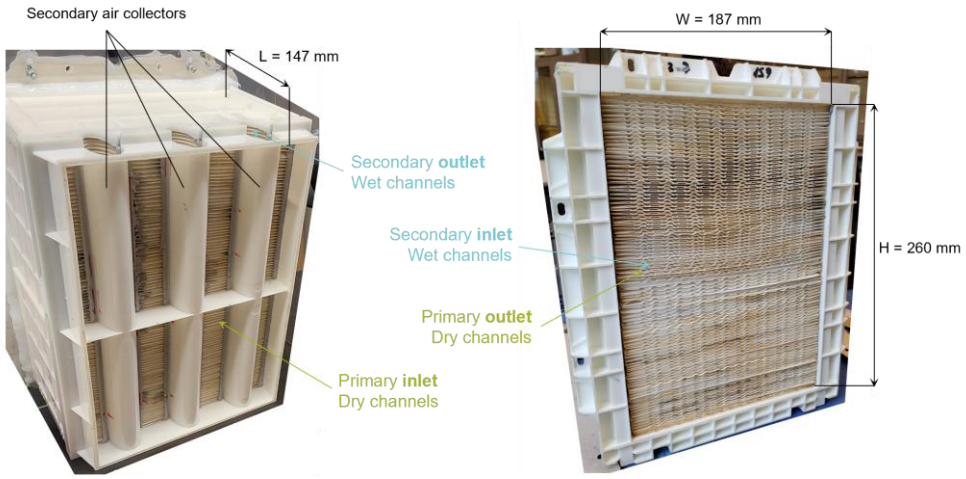

Figure 2. *Pictures of the front and back of the D-IEC to highlight dry and wet channels inlets and outlets.*

Figure 3 illustrates the integration of the D-IEC within the test bench. The air flows from the air ducts into a divergent, to ensure uniform air flow distribution at the D-IEC inlet. The primary air leaves the D-IEC on the left and is directed towards the air ducts with a convergent. The secondary extraction fan is located on the side of the D-IEC casing to avoid creating a preferential path towards the top or the bottom of the D-IEC. Water is supplied from the top of the D-IEC to both ends of its width at the entrance of the wet channels. Inside the D-IEC, water circulates through a sponge network driven by capillary and gravitational forces until it finally wets the whole surface of the linen sheets. The propagation of water inside the D-IEC is thus relatively slow.

The geometric characteristics of the D-IEC are given in Table 1. The D-IEC has been designed to operate with supply airflow rates from 45 to 150 m³/h to maintain laminar conditions in the dry channels while supplying a suitable airflow rate to the indoor environment.

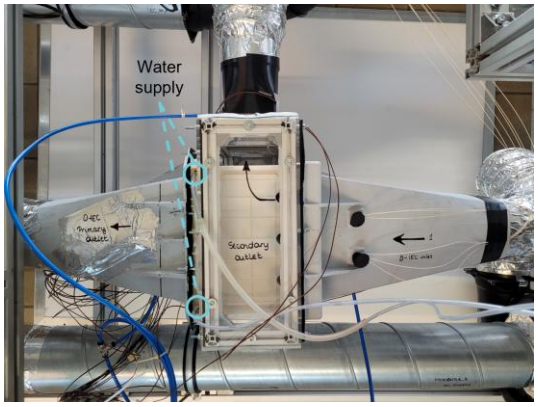

Figure 3. *Top view of the D-IEC casing, integrated within the test bench.*

Table 1. *D-IEC geometric characteristics.*

Characteristic	**Value**
Channel length	L = 147 mm
Channel width	W = 187 mm
Channel height	h_{ch} = 1.2 mm
Number of channels	200
D-IEC height	H = 260 mm
Wall material	Plastic with linen sheets coated on wet channels

2.1.2. Operating conditions

A realistic range of operating conditions has been defined using meteorological data of various climatic zones. Figure 4a shows the envelope of the outdoor conditions during the cooling season of the ten chosen climatic zones [22]. As developed in Section 1.2, the air entering the D-IEC is a mix of indoor (70%) and outdoor (30%)

air, thereby considerably reducing the operating range, as shown in Figure 4b. It has been assumed that the indoor environment is maintained at 23°C and 50% relative humidity.

The test bench is located in a room with small windows and no direct sunlight, ensuring relatively constant indoor conditions around 18-22°C with a humidity ratio of 6-8 g/kg. To avoid the need for air dehumidification and to meet the minimum expected humidity ratio at the D-IEC inlet, the minimum humidity ratio has been set to 6 g/kg. The minimum and maximum inlet temperatures have been set to 20 and 32°C respectively, and the maximum relative humidity to 72%, corresponding to 10-22 g/kg depending on the temperature.

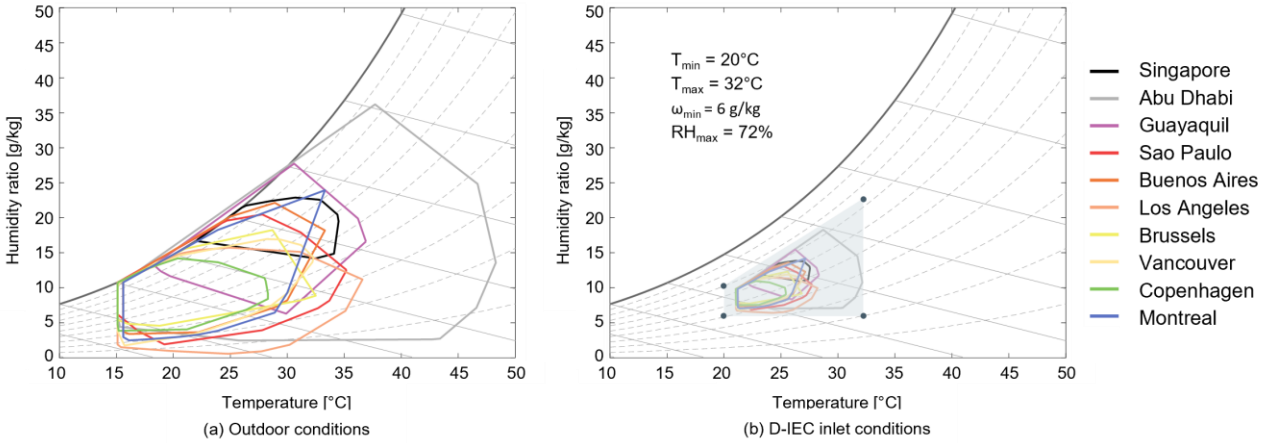

Figure 4. *Envelope of air conditions during cooling season for 10 climatic zones: (a) Outdoor air conditions (b) Air conditions at D-IEC inlet, after mixing with 70% of indoor air at 23°C and 50% relative humidity.*

2.2. Test bench P&ID

The complete test bench includes several components that modify the temperature and humidity of the air, until the desired conditions are reached at the D-IEC inlet. The P&ID of the test bench is presented in Figure 5a, while Figure 5b shows the evolution of the air conditions in the test bench components.

A fan (F1) sucks the ambient air into the ducts, where its temperature and humidity are measured with two sensors, for measurement cross-checking (states 1 and 2). The temperature and humidity of the air are modified through three components: first, an electrical heating resistor (HR1) sensibly heats the air (state 3); second, a direct evaporative cooler (DEC) humidifies the air (state 4) almost to saturation through direct evaporation of water into the air; finally, a second heating resistor (HR2) sensibly heats the air (state 5). The temperature and humidity at the D-IEC inlet can be adjusted by varying the power supplied to the heating resistors. In the dry channels of the D-IEC, the air is cooled sensibly (state 6) and is then rejected to the indoor environment through a second fan (F2). Part of the primary air is sucked into the wet channels through the third fan (F3). It leaves the D-IEC heated and humidified (state 7) and is rejected into the outdoor environment to avoid humidifying the room. The real installation is shown in Figure 6.

2.2.1. Components description

The *heating resistors* are used to heat the air flow sensibly. They produce heat by dissipating electrical energy via the Joule effect. The two heating resistors are controlled by a 0-10 V analogue signal that adjusts the current through them, dissipating power from 0 to 1800 W.

A *direct evaporative cooler* (DEC) cools the air through direct humidification. The core matrix of the DEC is made of a porous material. Water is supplied at the top of the DEC and flows down the corrugated sheets, where it infiltrates the porous material. The air enters the DEC perpendicularly and absorbs moisture as it flows through the cooler. The air is thus cooled and humidified when leaving the DEC.

The *fans* are centrifugal fans. Their main advantage is that they are equipped with volumetric airflow measurement, with an uncertainty of 1%. They have been installed at the D-IEC inlet and outlets to improve airflow control. Depending on the pressure losses of the installation, the provided volumetric flow rate can reach 800 m³/h.

A *peristaltic pump* is used to supply the D-IEC with water. A peristaltic pump is a positive-displacement pump that can deliver very low flow rates and offer a wide range of water flow rates by varying its rotational speed. The water is contained in flexible tubes fitted inside a circular pump casing. The rotor has a number of metal bars attached to its external circumference, which compress the flexible tubes as they rotate by. The part of the tube under compression is closed, forcing the water to move through the tube.

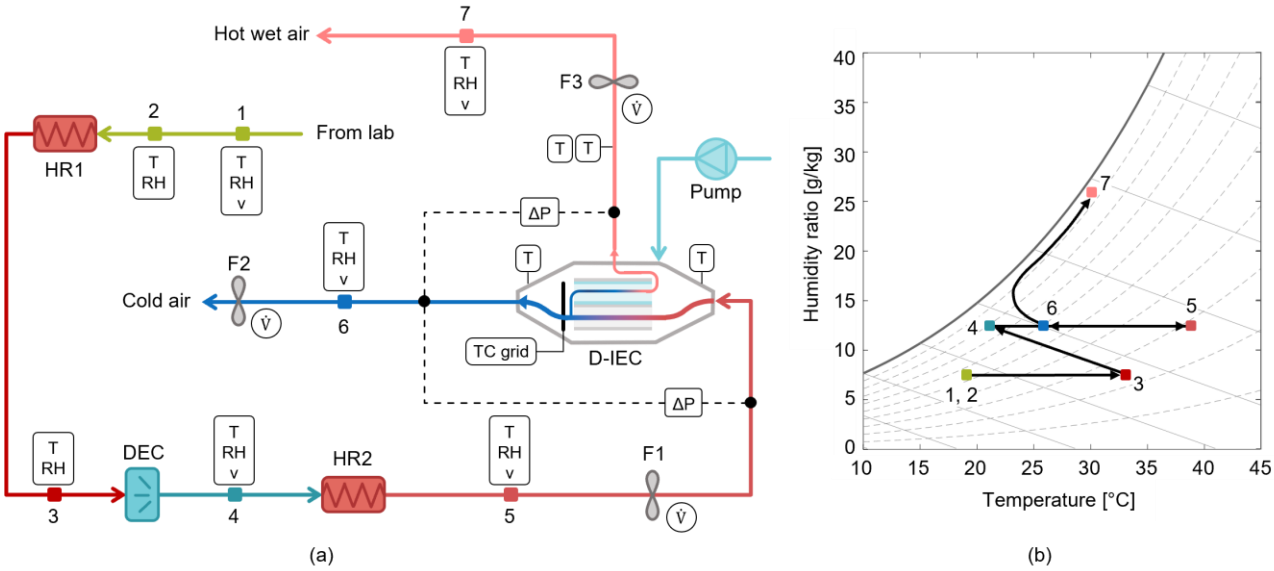

Figure 5. *(a) Test bench P&ID. (b) Evolution of the air conditions inside the test bench components.*

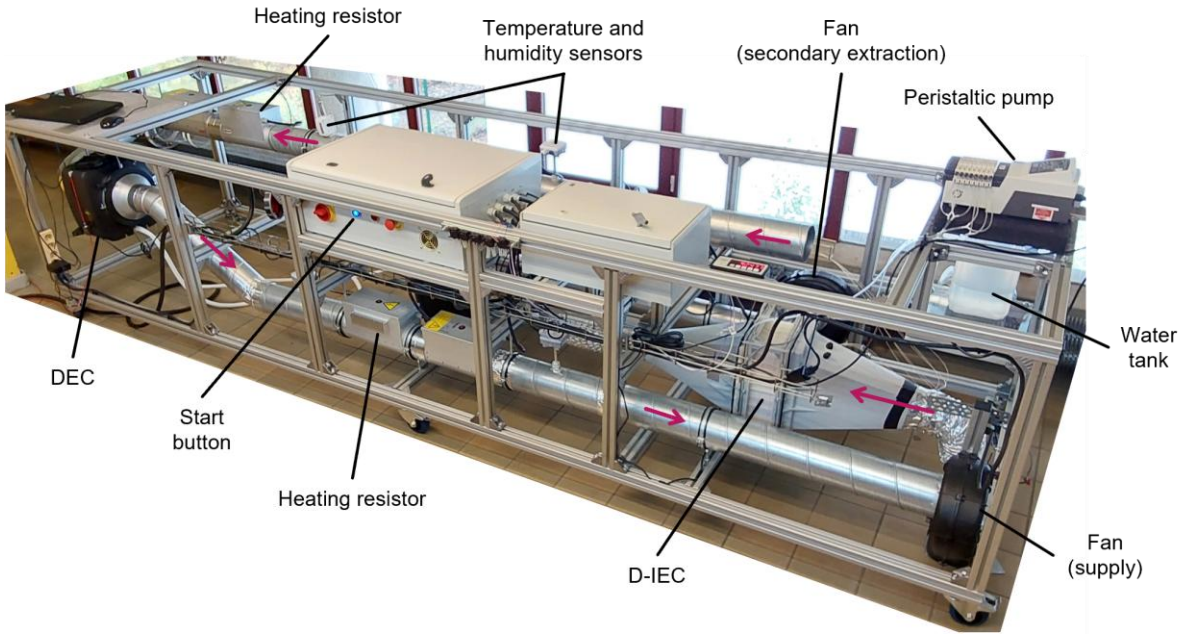

Figure 6. *Test bench picture highlighting its components. The pink arrows indicate the direction of airflow inside the test bench.*

2.2.2. Installation monitoring

The characteristics of the sensors used to monitor the air conditions in the test bench are given in Table 2. All sensors were provided with a calibration certificate. The data acquisition is managed through the LabVIEW software.

- Temperature and relative humidity are monitored at the seven identified air states.

- At the D-IEC inlet and outlets (states 5-7), the temperature is cross-checked using thermocouples. The airflow rate is provided by the inner sensor in the fans and can be cross-checked by computation from a punctual velocity measurement. The former is taken as the reference for airflow rate measurement because airflow computed from a punctual velocity yields large uncertainties.
- At the D-IEC primary outlet (state 6), a grid of 12 thermocouples monitors the temperature distribution across the evaporative cooler height.
- The humidity measurement can be cross-checked using sensors 4 to 6. Between those states, the air experiences only sensible heat transfer and the specific humidity should remain constant.

Table 2. *Summary of sensor characteristics.*

Sensor	**Measured quantity**	**Range**	**Accuracy**	**Location**
Senseca *HD29371TO1*	T RH v	-10 – 60 °C 0 – 100 % 0.2 – 10 m/s	± 0.3 K ± 1.5 % ± 0.5 m/s	1, 4-7
Senseca *HD4817TO1*	T RH	-20 – 80 °C 0 – 100 %	± 0.3 K ± 1.5 %	2, 3
Type T thermocouple	T	-50 – 350 °C	± 0.5 K	5-7
Ebmpapst *G3G190-RQ45-04* (centrifugal fan)	$\dot{V}$	10 – 400 m³/h	± 1.0 %	5-7
Sensirion SDP1108-R	ΔP	0 – 100 Pa 100 – 500 Pa	± 2.0 Pa ± 2.0 %	5-7

The measurement uncertainties of the temperature, relative humidity, and airflow rate can be propagated through an uncertainty analysis to evaluate their impact on computed quantities such as humidity ratio, heat transfer, or effectiveness, according to the reference international standard [23].

3. Commissioning

This section summarises the tests conducted prior to the first experimental campaign to ensure the validity of the measured results. All commissioning results are reported in Figure 7, and the methodology employed at each step is described below.

The water flow rate can be adjusted by varying the peristaltic pump's rotation speed, which ranges from 0 to 90 rpm. The water flow rate provided by the pump has been calibrated by weighing the water delivered over 60 seconds at increasing rotational speeds. As illustrated in Figure 7a, a linear regression could be derived for the water flow rate supplied by the pump.

The volumetric airflow rate is provided directly by the fans through dedicated software. The user can enter a desired flow rate, and the fan's actual airflow rate is displayed in the software. The flow rates predicted by the fans were cross-checked using pre-calibrated orifice plates (with 3% uncertainty) before building the test bench (Figure 7b).

Once the fans were mounted on the test bench at the D-IEC inlet and outlets, it could be verified that the fans indeed provided the specified volumetric airflow rate, provided mass balance was maintained. Although this is not proof that the D-IEC casing and the air ducts are completely airtight, particular attention was paid to ensuring airtightness at component intersections. The actual airtightness of the D-IEC casing could have been checked via pressurisation, but this was avoided given the materials used in the D-IEC and casing designs. There could also be internal leakage from the primary inlet directly to the secondary outlet, but because of the interconnection between the primary and secondary sides, there is currently no international standard for identifying it.

The head losses were measured at varying airflow rates across the D-IEC, without conditioning the air before it entered. The tests were performed under both dry and wet conditions to account for additional head losses due to wetting of the secondary channels. The secondary channels were wetted by supplying water at 1.5 L/min for 10 minutes. Then, a 45-minute wait was observed to ensure the water had spread evenly throughout the D-IEC. Figure 7c illustrates the evolution of the pressure losses in dry and wet conditions under various airflow rates. Under dry conditions and at similar airflow rates, head losses are greater in the secondary channels than in the primary channels. This is due to the additional U-turn of the air at the primary outlet,

returning to the D-IEC in the secondary channels, and to the vertical collectors at the secondary outlet, preventing mixing with the primary inlet.

Finally, the temperature and relative humidity measurements were cross-checked between the sensors by activating the fans to circulate air inside the test bench, but without conditioning it.

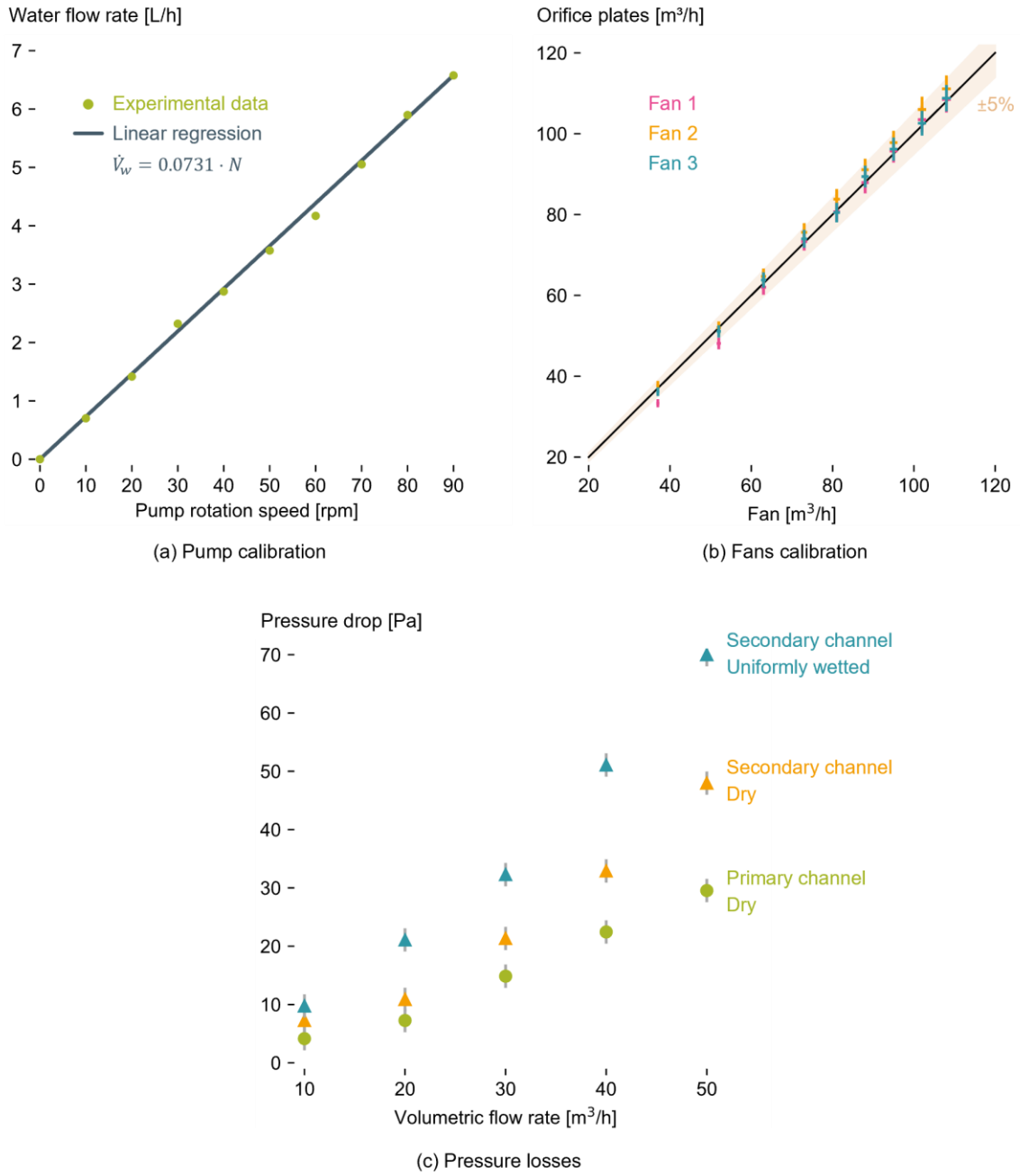

Figure 7. *Summary of commissioning results.*

4. Experimental results

The D-IEC was tested under the 6 operating conditions reported in Table 3. As mentioned in Section 2.1.1, water circulates through capillarity in the D-IEC, resulting in slow channels wetting. A general experimental procedure has been designed to ensure proper channel wettability:

1. *Soaking procedure*: The D-IEC is wetted with a high water flow rate for 10 minutes. Then, a 30-minute waiting period is observed to allow all the wet channels to soak up and let the excess water drain into a tank below the D-IEC. During the wetting procedure, there is no airflow inside the D-IEC.

2. The fans are activated such that the total airflow rate supplied to the D-IEC is 90 m³/h, and the extraction on the secondary outlet is 30 m³/h.
3. If necessary, the heating resistors HR1 and HR2, and the DEC are activated with the LabVIEW software to reach the desired supply conditions.
4. A 15-minute wait period is observed to ensure steady-state operation is reached. During this time, the water supply to the D-IEC is kept constant to compensate for evaporation, based on a water mass balance on the wet channels.

Two testing procedures were established to assess the experimental repeatability of the results under different wetting strategies. The difference between the two testing procedures lies in how the operating conditions are modified:

Test A. Steps 1-4 are applied under the first operating conditions (conditions *a* of Table 3), then the operating conditions are modified (conditions *b-f* of Table 3) by starting directly from step 3. The soaking procedure is not carried out between operating points.

Test B. Steps 1-4 are applied for all operating conditions (conditions *a-f* of Table 3). The soaking procedure is carried out between all operation points to ensure uniform wetting of the D-IEC.

The comparison between tests A and B enables the identification of variations in D-IEC behaviour with the wetting strategy and, possibly, the derivation of a water management strategy for long-term use.

Table 3. *Summary of tested operating conditions at the D-IEC inlet.*

	a	***b***	***c***	***d***	***e***	***f***
T [°C]	20	30	30	30	30	30
ω [g/kg]	6	6	9	11	12	13

The results obtained during Tests A and B are summarised in Figure 8. The temperature and humidity ratio at the inlet and outlets are consistent between both tests (Figure 8a and b). The results are repeatable as similar inlet conditions lead to similar outlet conditions on the primary and secondary sides.

The performance of the D-IEC can be assessed using wet-bulb (ε_{wb}) and dew-point effectiveness (ε_{dp}). Those indicators compare the temperature at the D-IEC primary outlet with the incoming air wet-bulb and dew-point temperatures, respectively (Figure 8c). For most operating conditions, the wet-bulb effectiveness is higher than 100%, meaning that the D-IEC is more performant than direct humidification. The dew-point effectiveness ranges from 50% to 80%, depending on operating conditions.

The energy balance between the primary and secondary sides remains within the uncertainty range (Figure 8d). It confirms that the D-IEC casing and the air ducts are airtight and that there are no leaks between the primary inlet and the secondary outlet under the current operating conditions.

The thermocouple grid measurements indicate that the temperature distribution at the D-IEC primary outlet is nonuniform along the D-IEC height during the test. The results reported in Figures 9 and 10 suggest that the wettability of the D-IEC can be investigated using thermocouple grids and pressure-drop measurements.

The results obtained during *Test A* (Figure 10) show that after one hour of continuous operation, the bottom of the D-IEC begins to dry out, as reflected by a temperature rise at the bottom of the D-IEC (45 mm height) and an overall decrease in the measured pressure drop on the secondary side.

During *Test B* (Figure 9), where the wetting procedure is carried out across all operating conditions, the channels in the upper half are flooded, preventing air from circulating through them. The primary air in contact with those channels is thus cooled only by sensible heat transfer with water, rather than by sensible and latent heat transfer, leading to higher outlet temperatures (155 and 215 mm height). The channels' flooding also increases the pressure drop on the secondary side because the air is distributed across fewer channels, which means it must circulate faster. After the second operating condition, a longer waiting time was observed to drain the excess water. When the tests were resumed, a uniform temperature distribution was observed at the D-IEC primary outlet. However, when the wetting procedure was repeated, wet-channel flooding was observed again.

The overall conclusions of the first experimental results can be summarised as follows:

- The testing procedure affects the internal behaviour of the D-IEC, as demonstrated by the thermocouple grid measurements, but it has a low overall impact on D-IEC performance.
- A 30-minute waiting time is not sufficient to drain all the excess water from the D-IEC.
- There could exist an optimal water management strategy that maximises the D-IEC performance. However, due to the complexity of the sponge network architecture, implementing such a water management strategy is not straightforward, as supported by the results of the two testing procedures.
- A suitable management strategy needs to be investigated if the system is to operate continuously in a building throughout the cooling period.

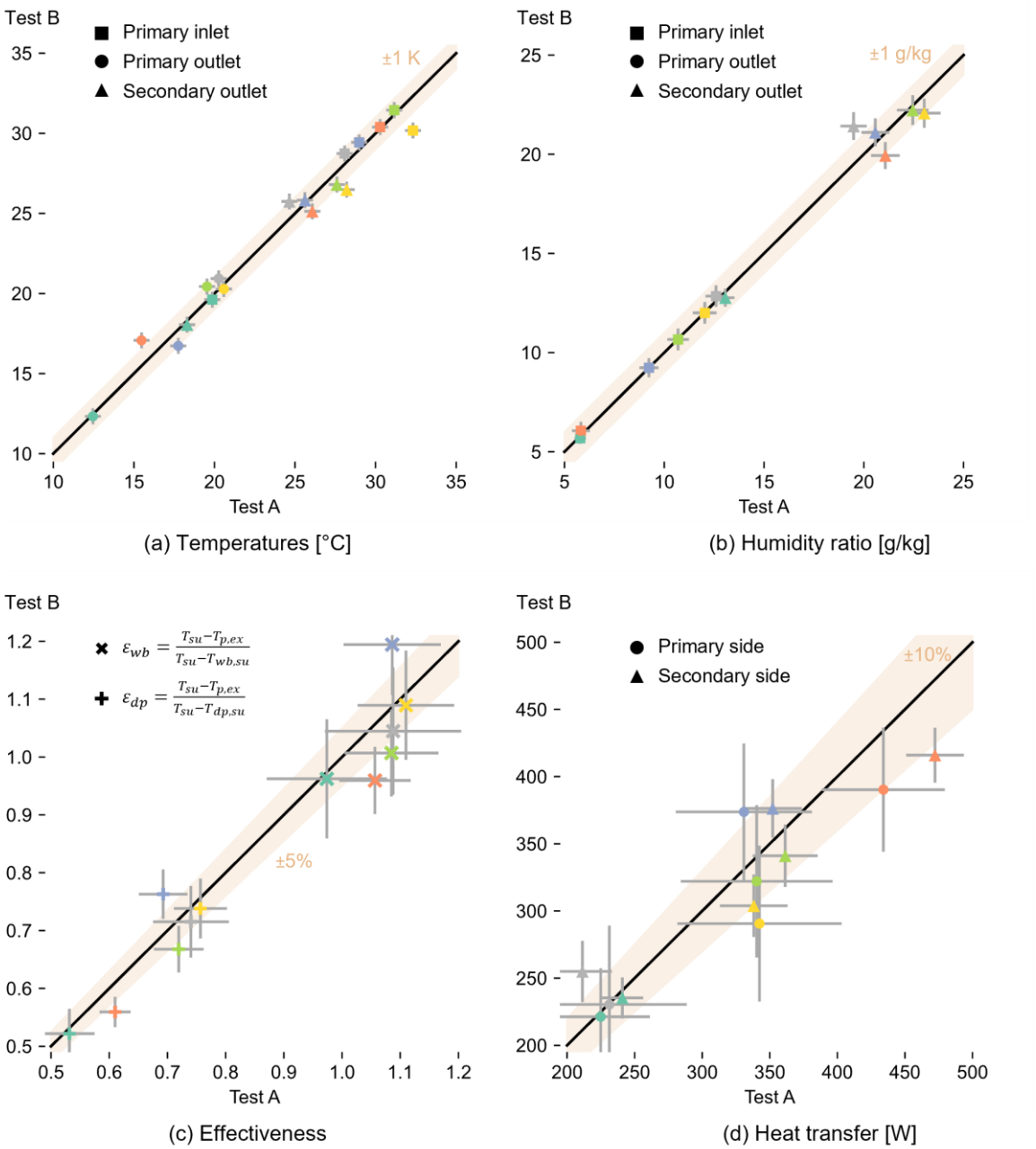

Figure 8. *Summary of repeatability results.*

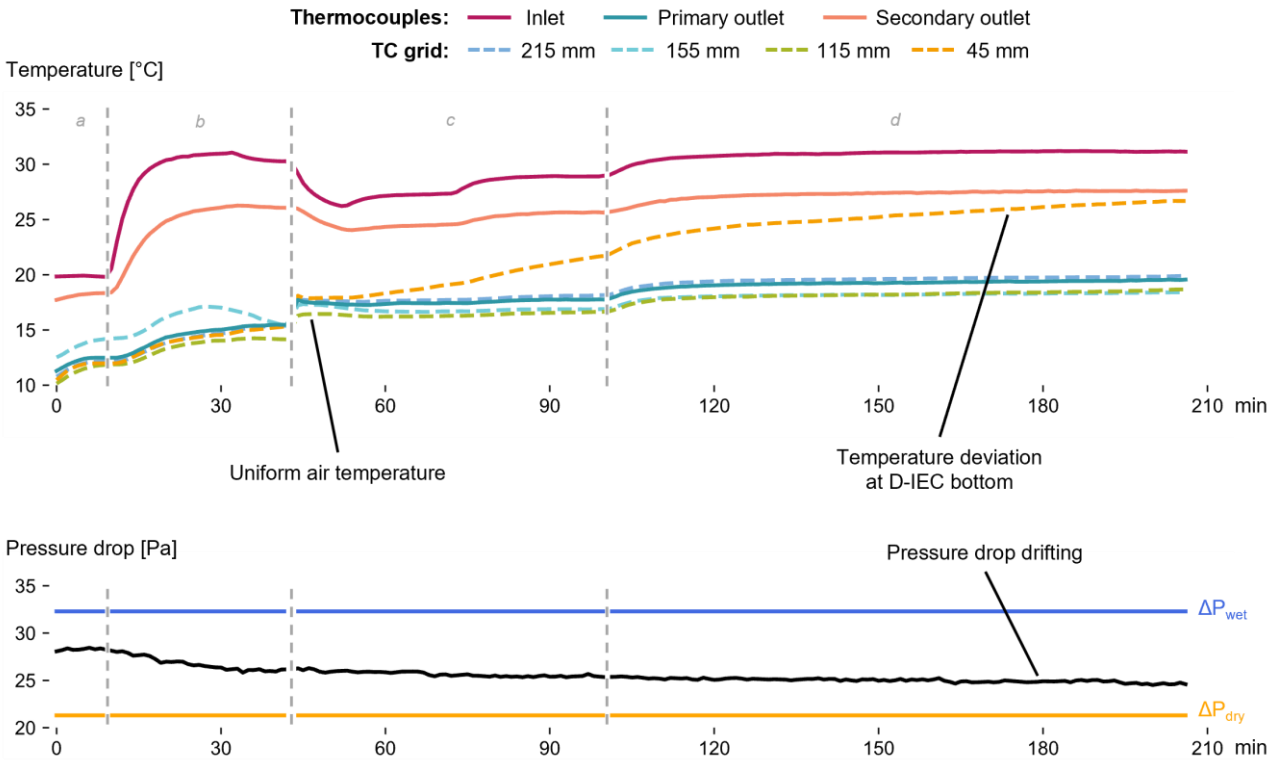

Figure 10. *Results of Test A for inlet air conditions a-d. The temporal evolution of the D-IEC outlet temperature measured by the thermocouple grid suggests that the bottom wet channels dry over time.*

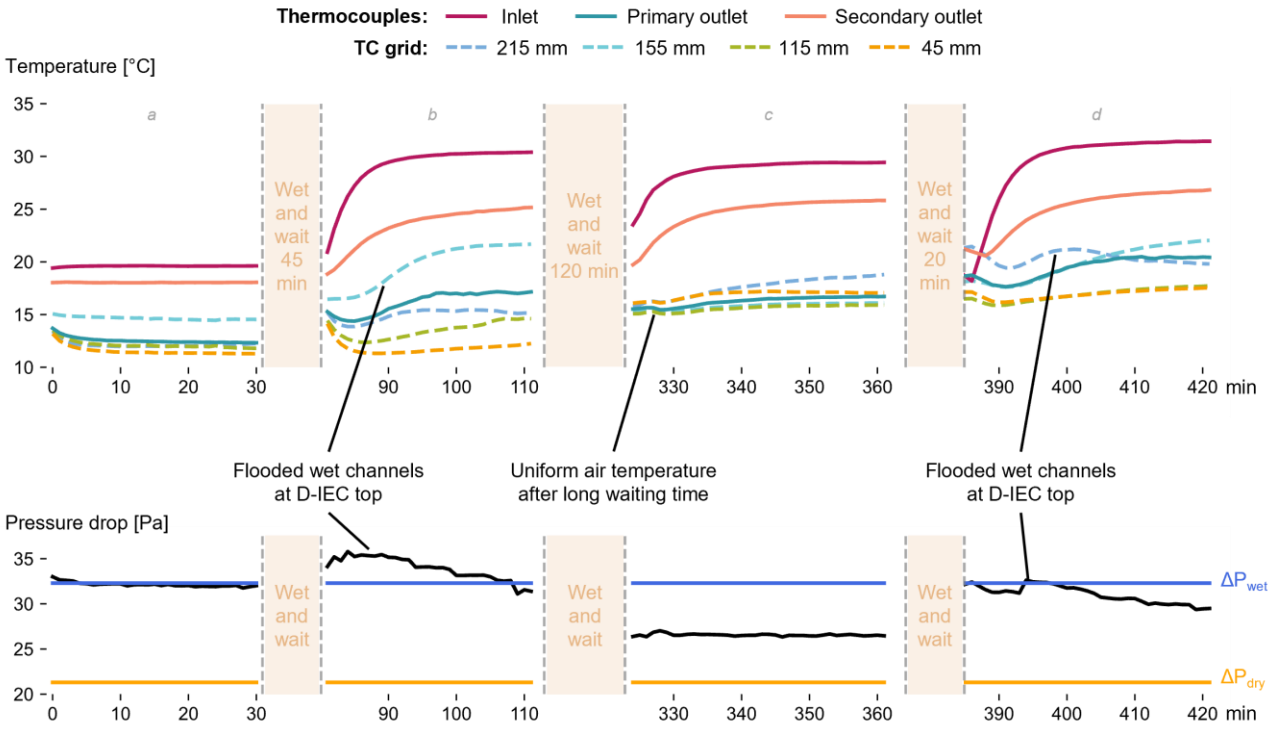

Figure 9. *Results of Test B for inlet air conditions a-d. The temporal evolution of the D-IEC outlet temperature measured by the thermocouple grid suggests that the top wet channels can be flooded if the water supply is too large.*

5. Conclusions

A D-IEC has been tested experimentally under various operating conditions to create a dataset suitable for validating evaporative cooler models on both the primary and secondary sides. This paper describes how the test bench was designed to achieve this goal, introducing the constraints related to the D-IEC geometric characteristics and intrinsic features, as well as the desired operating conditions. The architecture of the resulting test bench and its main components are described, and the installation monitoring is introduced. This paper also describes how the test bench was commissioned to ensure measurement validity before testing the D-IEC under various operating conditions.

An experimental campaign was led to establish the repeatability of the tests under two wetting strategies. In the first strategy, the wet channels were soaked at the beginning of the testing campaign to ensure uniform wetting. Then the water supplied to the D-IEC only replaced the water evaporated. Six operating conditions were tested during a total of three hours. After one hour of continuous operation, the bottom of the D-IEC began to dry. In the second strategy, wet channels were soaked between variations in operating conditions. However, this quickly led to channels flooding due to excess water.

Even though the two experimental procedures led to different inner behaviour of the D-IEC, the test's repeatability was ensured as similar inlet conditions resulted in similar outlet conditions for short-duration tests. This also suggests the existence of an optimal water management strategy to maximise D-IEC performance and ensure its long-term operation, which will be the subject of future investigation.

References

[1] De Cian E, Falchetta G., Pavanello F., Romitti Y., Sue Wing I., The impact of air conditioning on residential electricity consumption across world countries, J Environ Econs Manag 2025; 131:103122.

[2] European Foundation for the Improvement of Living and Working Conditions, Working conditions and workers' health, LU: Publications Office; 2019.

[3] Liu C., Kershaw T., Fosas D., Ramallo Gonzalez A., Natarajan S., Coley D., High resolution mapping of overheating and mortality risk, Build Env 2017; 122: 1–14.

[4] Carr D., Falchetta G., Sue Wing I., Population Aging and Heat Exposure in the 21st Century: Which U.S. Regions Are at Greatest Risk and Why?, The Gerontologist 2024; 64(3): 1-10.

[5] Park W., Shah N., Ding C., Qu Y., Challenges and Recommended Policies for Simultaneous Global Implementation of Low-GWP Refrigerants and High Efficiency in Room Air Conditioners, LBL Publications; 2019 Apr. Tech. Rep. OSTI ID: 1505528.

[6] Bezerra P., Da Silva F., Cruz T., Mistry M., Vasquez-Arroyo E., Magalar L., De Cian E., Lucena A. F., Schaeffer R., Impacts of a warmer world on space cooling demand in Brazilian households, Energ Build 2021; 234: 110696.

[7] Turek-Hankins L. L. et al., the Global Adaptation Mapping Initiative team, K. J. Mach, Climate change adaptation to extreme heat: a global systematic review of implemented action, Oxford Open Climate Change 2021; 1(1): kgab005.

[8] Intergovernmental Panel On Climate Change (Ipcc), Climate Change 2022 – Impacts, Adaptation and Vulnerability: Working Group II Contribution to the Sixth Assessment Report of the Intergovernmental Panel on Climate Change, 1st Edition, Cambridge University Press, 2023.

[9] Kiarsi M., Amiresmail M., Mahmoodi M. R., Farahmandnia H., Nakhaee N., Zareiyan A., Aghababaeian H., Heat waves and adaptation: A global systematic review, J Therm Bio 2023; 116: 103588.

[10] The Future of Cooling - Opportunities for energy efficient air conditioning, International Energy Agency; 2018.

[11] Porumb B., Unguresan P., Tutunaru L. F., Serban A., Balan M., A Review of Indirect Evaporative Cooling Technology, Energy Procedia 2016; 85: 461–471.

[12] Elnagar E., Pezzutto S., Duplessis B., Fontenaille T., Lemort V., A comprehensive scouting of space cooling technologies in Europe: Key characteristics and development trends, Renew Sustain Energy Rev 2023; 186: 113636.

[13] Cui Y., Zhu J., Zoras S., Liu L., Review of the recent advances in dew point evaporative cooling technology: 3E (energy, economic and environmental) assessments, Renew Sustain Energy Rev 2021; 148: 111345.

[14] Duan Z., Zhan C., Zhang X., Mustafa M., Zhao X., Alimohammadisagvand B., Hasan A., Indirect evaporative cooling: Past, present and future potentials, Renew Sustain Energy Rev 2012; 16(9): 6823–6850.

[15] Hsu S.T., Lavan Z., Optimization of wet-surface heat exchangers, Energy 1989; 14(11): 757–770.

[16] Anisimov S., Pandelidis D., Danielewicz J., Numerical analysis of selected evaporative exchangers with the Maisotsenko cycle, Energy Convers Manag 2014; 88: 426–441.

[17] Zeoli A., Gendebien S., Janod T., Moussa T., Maalouf C., Pacak A., Lemort V., Towards reliable model validation of evaporative coolers: Unified terminology and benchmark datasets, Appl Therm Eng 2026; 289: 129928.

[18] Lin J., Wang R., Li C., Wang S., Long J., Chua K.J., Towards a thermodynamically favorable dew point evaporative cooler via optimization, Energy Convers Manag 2020; 203: 112224.

[19] Riangvilaikul B., Kumar S., An experimental study of a novel dew point evaporative cooling system, Energy Build 2010; 42(5): 637–644.

[20] Liu Y., Akhlaghi Y.G., Zhao X., Li J., Experimental and numerical investigation of a high-efficiency dew-point evaporative cooler, Energy Build 2019; 197: 120–130.

[21] Pakari A., Ghani S., Regression models for performance prediction of counter flow dew point evaporative cooling systems, Energy Convers Manag 2019; 185: 562–573.

[22] Machard A. et al., Typical and extreme weather datasets for studying the resilience of buildings to climate change and heatwaves, Sci Data 2024; 11(1):531. 10.1038/s41597-024-03319-8.

[23] ISO IEC Guide 98-3, Uncertainty of Measurement—Part 3: Guide to Expression of Uncertainty in Measurement, International Organization for Standardization, ISO IEC Guide 98-3, Geneva Switzerland, 2008.